A New Concept for Humidity Sensing Using Curved Micro-beams

H Ouakad*, M. H Hasan** and F. Alsaleem***

*King Fahd University of Petroleum and Minerals, Dhahran, Saudi Arabia, houakad@kfupm.edu.sa
**University of Nebraska - Lincoln, NE, USA, mohammadhhasan@huskers.unl.edu
***University of Nebraska - Lincoln, NE, USA, falsaleem2@unl.edu

ABSTRACT

There are number of common humidity sensing methods in MEMS. They include capacitive, resistive, and thermal methods. Among these methods, capacitive sensing is considered the most common in MEMS. In this method, changes of a capacitor dielectric constant, due to the absorption of air water vapor into a coating layer is correlated to humidity. The slow sensor time response and the degradation of the coating material over time are the major limitations of this method. Humidity have recently been studied as significant sources for environmental noise that, if ignored while operating a typical MEMS sensor, may lead to poor performance. In this work, we propose the utilization of this effect to overcome the challenging limitations of the humidity capacitive sensing. Specifically, we propose the use of an uncoated arch micro-beam to detect changes in the thermal properties of air due to humidity. Found to amplify these changes by orders of magnitude due to the richness of its nonlinear dynamics, an arch beam was selected for this investigation. These amplified effects become the measurements of interest, rather than being treated as noise. This new way of sensing humidity, can eliminate the need for the coating layer and significantly decrease the sensor response time.

Keywords: Humidity, MEMS, Squeeze-Film-Damping, Arched microbeam, non-coated

1 INTRODUCTION

Resistive and capacitive-based sensing technologies were proposed to measure humidity. Capacitive sensing, the most common [1], relies on the change of the dielectric constant of the sensor due to the changes of air properties, absorption of moisture into the sensing element, a chemical reaction between the sensing element and the moisture, or a combination of the three. Due to their mass production and low power requirement, MEMS devices are becoming more popular for sensing humidity. Static [1] [2] and dynamic excitation [3] are the most common operating modes for MEMS humidity sensors and other sensing approaches, such as mass and gas sensing [4]. MEMS humidity sensors are typically coated by polymer or ceramic materials. Those ceramics usually have limited life [5-7] or a have a low sensing range [8]. In this work we demonstrate the use of an uncoated MEMS resonator to measure humidity. The changes in thermo-electrical air properties due to humidity variation will be tracked and correlated to humidity. A few studies have shown that MEMS resonator characteristics could change as the thermal conditions of air varies [9-11]. However, those effects were seen as disturbances. In this study, we show that these thermal condition effects on a MEMS resonator could be, alone, used as humidity measurement signals. Thus, eliminating the need for a coating layer, increasing the expected lifespan of humidity sensors, and significantly reducing their degradability.

The organization of this paper is as follows: In section 2, we present the mathematical model for this system. In section 3, show some simulation results and discussion. Finally, we conclude with conclusion and ongoing work in section 4.

2 MATHEMATICAL MODEL

The proposed MEMS sensor is illustrated in Figure 1. It consists of a clamped-clamped arched microbeam with length $l\ (m)$, width $b\ (m)$, thickness $h\ (m)$. The microbeam is separated from the substrate underneath it by an initial gap $d\ (m)$ and has an initial profile $w_0(x)\ (m)$.

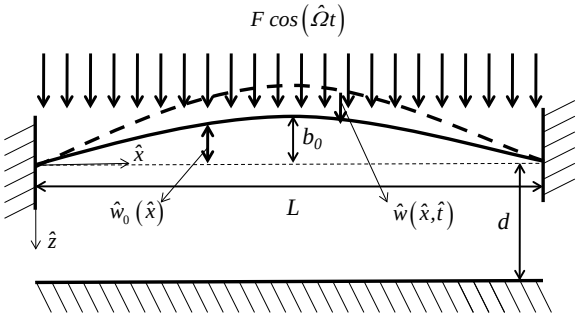

Figure.1: Arched micro-beam model. The beam vibrates about its z-axis. Snap-through occurs when the beam's oscillation is about the dashed line.

The microbeam is actuated by a sinusoidal electrostatic force, which oscillate the microbeam. The equation of motion of the microbeam is given by equation (1) and the initial and boundary conditions are given in (2):

$$EI_c\frac{\partial^4 w}{\partial x^4}+\rho A\frac{\partial^2 w}{\partial t^2}+F_d(x,t)=\left(\frac{\partial^2 w}{\partial x^2}-\frac{d^2 w_0}{dx^2}\right)*\left[\frac{EA}{2l}\int_0^l\left\{\left(\frac{\partial w}{\partial x}\right)^2-2\left(\frac{\partial w}{\partial x}\frac{dw_0}{dx}\right)\right\}dx-N\right]+F(t)\ \ldots(1)$$

$$w(0,t)=w(l,t)=0$$

$$\frac{\partial w(0,t)}{\partial t}=\frac{\partial w(l,t)}{\partial t}=0\ \ldots(2)$$

where E is the Young modulus of elasticity (Pa), I_c is the second moment of area of the rectangular cross section of the micobeam about its center of mass (m^4), x is the postion along the length of the microbeam (m), $w(x,t)$ is the deflection of the microbeam, t is the time (s), ρ is the density of the microbeam (kg/m^3), A is the cross-sectional area of the microbeam $A=lb\ (m^2)$, $F_d(x,t)$ is the drag force of air acting on the microbeam per unit length (N/m), N is the axial force acting at the microbeam per unit length (N/m), and $F(t)$ is the external excitation force per unit length (N/m).

The drag (damping) force in equation (1) is due to the microbeam interaction with the surrounding air. This force dissipates most of the microbeam's energy, which dampens its vibration. Because of the size of the microbeam and the substrate underneath it, most energy is dissipated through squeeze-film damping [12]. The drag force acting on the microbeam is calculated by:

$$F_d=\int_0^b(P(x,y,t)-P_a)dy\ \ldots(3)$$

where $P(x,y,t)$ is the pressure distribution at the bottom surface of the microbeam (Pa), P_a is the ambient pressure (Pa), and y is the lateral position along the microbeam (μm). The pressure distribution can be approximated using equation (4) when the gap (d) is much smaller than the width and length of the microbeam [13].

$$\frac{\partial}{\partial x}\left(\frac{\rho_a(d-w+w_0)^3}{12\mu}\frac{\partial P}{\partial x}\right)+\frac{\partial}{\partial y}\left(\frac{\rho_a(d-w+w_0)^3}{12\mu}\frac{\partial P}{\partial y}\right)=\frac{\partial}{\partial t}\left(\rho_a(d-w+w_0)\right)\ldots(4)$$

with the following boundary conditions:

$$P(x,y=0)=P(x,y=b)=P_a$$

$$\frac{\partial P(x=0,y)}{\partial x}=\frac{\partial P(x=l,y)}{\partial x}=0$$

where ρ_a is the density of air (Kg/m^3) and μ is the dynamic viscosity constant of air $(Pa.s)$. The internal axial stress is assumed to be zero. Dimensional analysis is performed on equations (1) and (3) using the following dimensionless variables:

$$\hat{x}=\frac{x}{l},\quad \hat{w}=\frac{w}{d},\quad \widehat{w_0}=\frac{w_0}{d},\quad \hat{t}=\frac{t}{T},\quad \hat{P}=\frac{P}{P_a},\quad \hat{y}=\frac{y}{b}\ \ldots(6)$$

where T is the time constant of the system defined as $T=\sqrt{\frac{\rho Al^4}{EI_c}}$. Using the nondimensional variables in (6) and dropping the hat for convenience, equations (1), (2), (3) become:

$$w_0(x,t)=\frac{b_0}{2d}[1-\cos(2\pi x)]\ \ldots\ldots\ (7)$$

$$\frac{\partial^4 w}{\partial x^4}+\frac{\partial^2 w}{\partial t^2}+\widehat{F_d}(x,t)=\alpha_s\left(\frac{\partial^2 w}{\partial x^2}-\frac{d^2 w_0}{dx^2}\right)\left[\int_0^1\left\{\left(\frac{\partial w}{\partial x}\right)^2-2\left(\frac{\partial w}{\partial x}\frac{dw_0}{dx}\right)\right\}dx-N_{non}\right]+\hat{F}(t)\ \ldots\ldots\ldots\ldots\ (8)$$

with the following boundary conditions:

$$w(0,t)=w(1,t)=0$$

$$\frac{\partial w(0,t)}{\partial t}=\frac{\partial w(1,t)}{\partial t}=0$$

and $\widehat{F_d}=\int_0^1(P(x,y,t)-1)dy\ \ldots(9)$

$$\frac{d^2}{l^2}\frac{\partial}{\partial x}\left(\frac{(1-w+w_0)^3}{\mu}\frac{\partial P}{\partial x}\right)+\frac{d^2}{b^2}\frac{\partial}{\partial y}\left(\frac{(1-w+w_0)^3}{\mu}\frac{\partial P}{\partial y}\right)=-\frac{12}{P_aT}\frac{\partial w}{\partial t}\ldots(10)$$

with the following boundary conditions:

$$P(x,y=0)=P(x,y=1)=1$$

$$\frac{\partial P(x=0,y)}{\partial x}=\frac{\partial P(x=1,y)}{\partial x}=0$$

where $\widehat{F_d}(x,t)$, $\hat{F}(t)$ and N_{non} are the nondimensional drag force, external force, and axial stress, respectively and the nondimensional parameter $\alpha_s=6\left(\frac{d}{h}\right)^2$. It was shown that, for a microbeam that satisfies $l\gg b\gg d$, the pressure distribution solution for equation (3) is given by [14]:

$$P(x,y,t)=1+\frac{6\mu_{eff}b^2}{P_aTd^2(1-w+w_0)^2}(y-y^2)\frac{\partial w}{\partial t}\ldots(11)$$

where μ_{eff} is the effective dynamic viscosity, a modified value of the viscosity constant to account for the slip at the boundary layer and allows the no-slip analysis, $\mu_{eff}=\frac{\mu}{1+6Kn}$, Kn is the Knudsen number which is given by $Kn=\lambda_a/(d-w+w_0)$, λ_a is the mean free path of air molecules at the operating ambient pressure (nm) and is given by $\lambda_a=\lambda_0P_0/P_a$, P_0 is the atmospheric pressure $(101.325\ KPa)$, and λ_0 is the mean free path at atmospheric pressure $(65\ nm)$.

Temperature and humidity are affecting the drag force $(\hat{F}_d)$ through changes in μ and therefore μ_{eff}. These effects are described by [15]:

$$\mu_m = \frac{\mu_a(1-X)}{[(1-X)+X*\Phi_{av}]} + \frac{[X*\mu_v]}{[(X)+(1+X*\Phi_{va})]} \quad \ldots (12)$$

where μ_m is the dynamic viscosity of humid air at a given temperature, X is the absolute humidity of vapor in air, Φ_{av} and Φ_{va} are interaction parameters between dry air and water vapor and can be calculated as:

$$\Phi_{av} = \frac{\sqrt{2}}{4}\left(1+\frac{M_a}{M_v}\right)^{-0.5}\left[1+\left(\frac{\mu_a}{\mu_v}\right)^{0.5}\left(\frac{M_v}{M_a}\right)^{0.25}\right]^2 \quad \ldots (13)$$

$$\Phi_{va} = \frac{\sqrt{2}}{4}\left(1+\frac{M_v}{M_a}\right)^{-0.5}\left[1+\left(\frac{\mu_v}{\mu_a}\right)^{0.5}\left(\frac{M_a}{M_v}\right)^{0.25}\right]^2 \quad \ldots (14)$$

where M_a and M_v are the molar mass of dry air and water vapor (kg/mol), respectively, μ_a is the viscosity constant of dry air and μ_v is the viscosity of water vapor and are given by:

$$\mu_a = MA_0 + MA_1(\Theta_a + 273) + MA_2(\Theta_a + 273)^2 + MA_3(\Theta_a + 273)^3 + MA_4(\Theta_a + 273)^4 \ldots (15)$$

$$\mu_v = (MV_0 + MV_1\Theta_a) \ldots (16)$$

where MA_i and MV_i are interpolating constants.

The system of equations describing the MEMS dynamics are then solved using the Galerkin method [14].

3 RESULTS AND DISCUSSION

A microbeam with length $l = 1000\mu m$, width $b = 30\mu m$, thickness $h = 2.4\mu m$, initial gap $d = 10.1\mu m$, density $\rho = 2332\ Kg/m^3$, Young's modulus $E = 166GPa$, axial stress N =0, an initial rise $b_0 = -3.5\mu m$ is used in this investigation. The negative sign denotes a downward initial curvature.

Figure.2 shows the linear response of the micro-beam around its natural frequency as a function of humidity at a constant ambient temperature. The natural frequency of the micro-beam shifts to the left as the relative humidity increases. A shift of about 33 Hz can be observed over the full range of humidity. In addition, the oscillation amplitude increases as the relative humidity increases (0.03µm, around 8% increase). These changes in the beam oscillation and frequency can be used to measure humidity as shown in Figure.3. Under sufficiently high voltages, the beam buckles through its center and "snap-through" occurs. Figure.4 shows the snap-through phenomenon around the beam's third natural frequency. A frequency shift of about 290 Hz over the full range of humidity occurs. This is a nearly 1350% increase over the linear resonance. Snap-through can also occur around the beam's first natural frequency, but with only one-third of that frequency shift around the full range of humidity. These results are summarized in Figure.5.

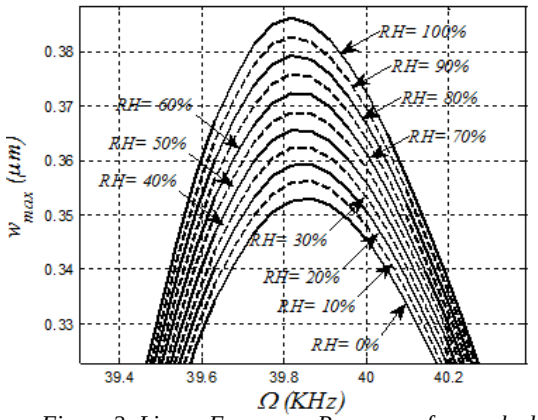

Figure.2: Linear Frequency Response of an arched beam around its natural frequency at $60°C$.

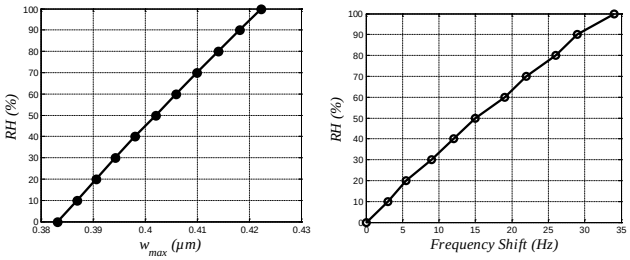

(a) *(b)*

Figure.3: Relative humidity effect is almost linear with (a) beam deflection or (b) frequency

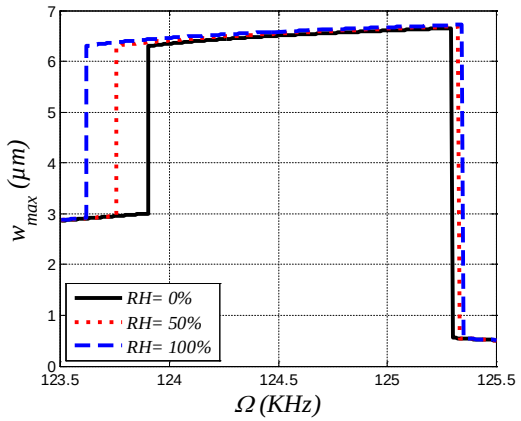

Figure.4: Snap-through frequency response of an arched beam around its third natural frequency

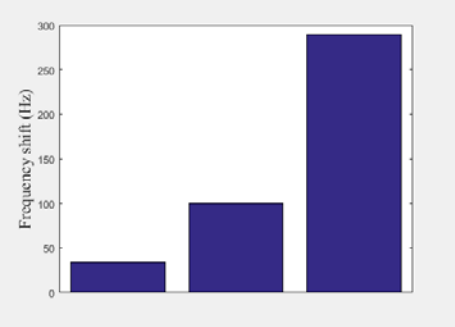

Figure.5: The arched beam frequency shift over the full range of humidity with different excitation scenarios

4. CONCLUSION

In this work, we showed a new capacitive MEMS sensor concept using an uncoated, curved microbeam beam. The concept relies on the effects of the water content in air on the overall dynamic damping in the MEMS structure. As relative humidity increases, the water content increases and the system's damping decreases. This results in a frequency shift. This frequency shift is an indication to the water content in the ambient air. Furthermore, we showed that it is possible to amplify the sensor response by nonlinear actuation.

REFERENCES

[1] Okcan, B., & Akin, T. "A low-power robust humidity sensor in a standard CMOS process". IEEE Transactions on Electron Devices, 54(11), 3071-3078. (2007).

[2] Lee, Y., & Lee, B. "Micromachine-based humidity sensors with integrated temperature sensors for signal drift compensation". Journal of micromechanics and microengineering, 13(5), 620. (2003).

[3] Penza, M., & Cassano, G. "Relative humidity sensing by PVA-coated dual resonator SAW oscillator". Sensors and Actuators B: Chemical, 68(1), 300-306. (2000).

[4] Bedair,S., & Fedder, K. "CMOS MEMS oscillator for gas chemical detection". In Sensors, 2004. Proceedings of IEEE , 955-958. IEEE. (2004)

[5] Chen, Z., & Lu, C. "Humidity sensors: a review of materials and mechanisms". Sensor letters, 3(4), 274-295. (2005).

[6] Ralston,K., Buncick, C., Denton, D., Boltshauser, E., Funk, M., & Baltes, P. "Effects of aging on polyimide: a model for dielectric behavior (of relative humidity sensors). In Solid-State Sensors and Actuators". Digest of Technical Papers, TRANSDUCERS'91. International Conference IEEE. 759-763. (1991).

[7] Dameron,A., Davidson, D., Burton, B., Carcia, F., McLean, S., & George, M. "Gas diffusion barriers on polymers using multilayers fabricated by Al2O3 and rapid SiO2 atomic layer deposition". The Journal of Physical Chemistry C, 112(12), 4573-4580. (2008).

[8] Jachowicz, R., & Weremczuk, J. "Sub-cooled water detection in silicon dew point hygrometer". Sensors and Actuators A: Physical, 85(1), 75-83. (2000).

[9] Hosseinian, E., Theillet, O., & Pierron, N. "Temperature and humidity effects on the quality factor of a silicon lateral rotary micro-resonator in atmospheric air. Sensors and Actuators" A: Physical, 189, 380-389. (2013).

[10] Jianqiang, H., Changchun, Z., Junhua, L., & Yongning, H. "Dependence of the resonance frequency of thermally excited microcantilever resonators on temperature". Sensors and Actuators A: Physical, 101(1), 37-41. (2002).

[11] Jan, T., Ahmad, F., Hamid, B., Khir, M., Shoaib, M., & Ashraf, K. "Experimental investigation of temperature and relative humidity effects on resonance frequency and quality factor of CMOS-MEMS paddle resonator". Microelectronics Reliability. (2016).

[12] Starr, B., "Squeeze-film damping in solid-state accelerometers", in Proceedings of the IEEE Solid-State Sensor and Actuator Workshop, Hilton Head Island, SC, 44–47 (1990).

[13] Hosaka, I. "Damping characteristics of beam-shaped micro-oscillators". Sensors and Actuators A: Physical, 87-95 . (1995).

[14] Ouakad, H.-Q. "Influence of squeeze-film damping on the dynamic behavior of a curved micro-beam". Advances in Mechanical Engineering. (2016).

[15] Tsilingiris, P. "Thermophysical and transport properties of humid air at temperature range between 0 and 100 C". Energy Conversion and Management, 1098-1110. (2008).